HUNGARIAN JOURNAL OF
INDUSTRY AND CHEMISTRY
Vol. 51(2) pp. 7–14 (2023)
hjic.mk.uni-pannon.hu
DOI: 10.33927/hjic-2023-12

EFFECT OF HEAT TREATMENT ON THE STRUCTURE OF SELF-ASSEMBLED UNDECENYL PHOSPHONIC ACID LAYERS DEVELOPED ON DIFFERENT STAINLESS STEEL SURFACES

ÉVA KOCSISNÉ PFEIFER[1], JÁNOS MINK[2], ISTVÁN GÁBOR GYURIKA[1] AND JUDIT TELEGDI[2,3*]

[1] Institute of Materials and Mechanical Engineering, University of Pannonia, Egyetem u. 10, Veszprém, 8200, HUNGARY
[2] Institute of Materials and Environmental Chemistry, Research Centre for Natural Sciences, Magyar tudósok körútja 2, Budapest, 1117, HUNGARY
[3] Faculty of Light Industry and Environmental Engineering, Óbuda University, Doberdó út 6, Budapest, 1034, HUNGARY

Deterioration caused by corrosion is well known, which can destroy metallic and non-metallic materials alike. Dissolved inhibitors of bionic micro- and nanocoatings can decrease the degree of undesirable corrosion in various ways. In this paper, a self-assembled molecular layer formed from undecenyl phosphonic acid developed on two different steel surfaces was the subject of our experiments. The influence of the metal composition, layer-forming conditions and post-heat treatment was documented by wettability measurements as well as surface roughness parameters; the change in surface morphology caused by the formation of a layer in addition to post-heat treatment was visualized by an atomic force microscope (AFM); and infrared spectroscopy elucidated the bindings of the amphiphilic molecules involved in the self-assembled layer to the metal surface as well as to each other. Over the course of the self-assembling process, the $-P(O)(OH)_2$ head groups can fix the amphiphilic molecule to the solid surface through the metal oxide-hydroxide layer. The hydrophobic alkenyl chains remain together as a result of special forces, namely hydrogen bonds and van der Waals forces, between them. The double bond at the end of the alkenyl chain disturbs how well the layer is ordered. To improve the homogeneity of the molecular layer and increase its level of compactness, the self-assembled molecular (SAM) layer was heat treated to achieve a more compact molecular film that can perfectly cover the metal surface.

Keywords: alkenyl phosphonic acid, self-assembled layer, wettability, surface morphology, atomic force microscope, infrared spectroscopy

1. Introduction

Since corrosion is a major problem, the development of effective corrosion inhibitors in many industrial sectors is important. The use of organic inhibitors has been extensively studied and several classes of inhibitors developed for different metals as well as in various environments. Among the various types of corrosion inhibitors, organic compounds with heteroatoms such as oxygen, nitrogen, phosphorous and/or sulfur are commonly used due to their high adsorption capability on a metal surface, which is mainly due to the lone pairs of electrons on the heteroatoms [1]-[2]. For the corrosion inhibition of iron, phosphonic acid derivatives are applied in different aqueous and oily environments, not only in dissolved form but as additives in coatings, concrete, etc. These molecules are stable as the covalent bond between the phosphorous and carbon atoms stabilizes the molecule, so these molecules are not nutrients for micro- and macroorganisms, that is, they do not increase the degree of eutrophication of natural waters. Alkyl and aralkyl phosphonic acids as well as their substituted derivatives form an effective class of organic inhibitors applied in both neutral or acidic media.

Numerous studies have reported the effectiveness of alkyl phosphonic acids as corrosion inhibitors of various metals, including steel, aluminum, copper and zinc. For example, a very good review article summarizes the usefulness of phosphonic acids as inhibitors to control the corrosion of mild steel in acidic environments by providing information about the enhanced inhibition efficiency at increased concentrations attributed to the adsorption of the inhibitor molecules [3]. Similarly, a good review article on the inhibition of copper corrosion by alkyl phosphonic acids attributed to the adsorption of inhibitor molecules to the copper surface has been published [4]. Alternatively, phosphonates [5] or phosphonic acid inhibitors can be used when they are embedded in nanolayers as several publications have demonstrated, e.g. on aluminum [6], iron [7] or titanium [8] and copper alloys [9]-[10] amongst other possible applications.

Received: 22 July 2023; Revised: 14 August 2023;
Accepted: 14 August 2023
*Correspondence: telegdi.judit@ttk.hu

The adsorption behavior of alkyl phosphonic acids on metal surfaces has been investigated using various techniques, including electrochemical impedance spectroscopy, atomic force microscopy and X-ray photoelectron spectroscopy. These studies demonstrated that the molecules of alkyl phosphonic acid adsorb onto the metal surface through a combination of chemisorption and physisorption mechanisms. The chemisorption mechanism involves the formation of a covalent bond between the inhibitor molecule and the metal surface, while the physisorption mechanism involves weak van der Waals forces between the inhibitor molecule and the metal surface. It is important to emphasize that although the head group of these amphiphilic molecules is bound to the solid surface, the metal oxide layer is never bound directly to the pure metal.

The effect of the alkyl chain length on the inhibition efficiency of alkyl phosphonic acids has also been studied. It has been reported that the inhibition efficiency rises as the alkyl chain length increases up to a certain point after which it starts to decrease. Even though it is not easy for a shorter amphiphile to form a homogenous nanolayer, molecules with longer hydrophobic chains form compact molecular films over a shorter period of time, which is attributed to stronger hydrophobic interactions between the alkyl/aralkyl chains. A homogenous, compact nanolayer can better control the corrosion processes as the aggressive ions cannot get close to the metal surface [10]-[12].

In addition to the anticorrosion activity, alkyl phosphonic acids exhibit other useful properties such as surfactant behavior and the ability to form stable lamellar structures in aqueous media that are advantageous in various applications such as when synthesizing nanocomposites.

One method of increasing the compactness of self-assembled molecular layers (SAMs) is by heat treating those that have already formed on different solids to help remove water molecules that have formed during the adsorption of phosphonic acid functional groups as well as eliminate the residual solvent. As a result, the van der Waals forces and hydrogen bonding between the alkyl/alkenyl chains increase. In the case of the double bond in the hydrophobic side chain, heat treatment could facilitate the polymerization of amphiphilic molecules involved in the SAM layer. The proximity of the unsaturated bonds in the nanofilm allows polymerization to take place in the absence of any other additives/catalysts. It is important to take into consideration the heat sensitivity of the molecules that are found in the SAM film. Several examples are found in the literature of when the positive influence of heat treatment not only influences layer formation but confirms the structure of the nanolayer, e.g. in the case of a copper alloy [9] and on mica [13]. In all cases, the aim was to reduce the number of pores formed in phosphonic acid layers by changing their conformation.

These examples in the literature prove the effectiveness of alkyl/aralkyl phosphonic acid nanolayers on a wide range of metals. In this paper, the nanolayer formation of undecenyl phosphonic acid on two different iron alloys is demonstrated and the possibility of improving the effectiveness of this special alkenyl phosphonic acid in the formation of compact nanolayers addressed. The questions raised were: 1) How can the alloying metal components influence the formation of self-assembled molecular layers?; and 2) Will the compactness of the nanolayer be improved by post-treatment or not? Furthermore, layer formation was analyzed by infrared spectroscopy [5].

2. Experimental

2.1. Solid supports

In our experiments, two types of stainless steel were used with the following compositions: 1) 1.4841: elements [%]: Cr: 25, C: 0.2, Si: 2, Mn: 2, P: 0.045, S: 0.045, balance Fe; 2) 1.4571: elements [%]: Cr: 17, C: 0.08, Si: 1, Mn: 2, P: 0.045, S: 0.045, Mo: 2, Ni: 12, Ti: 0.7, balance Fe.

The metal samples (10x10x1 mm) were smoothened with emery paper (200, 400, 800, 1200 mesh) and polished with diamond pastes (grain size: 15, 12, 9, 6 and 3 μm). All polishing treatments were followed by sonicating the coupons as well as washing them in water and finally with methanol.

2.2. Amphiphile

In all the experiments, undecenyl phosphonic acid ($CH=CH-[CH_2]_9-PO(OH)_2$, MW: 234) (Specific Polymers, Castries, France) was used to form the SAM layer. A solution of $5x10^{-3}$ M amphiphile was prepared by dissolving it in methanol.

2.3. Self-assembled molecular layer (SAM) preparation

The metal coupons were immersed in the solution of undecenyl phosphonic acid at 23°C for different periods of time, namely 4, 24 and 48 hours. Following immersion, the metal samples were rinsed in pure methanol to remove the excess of amphiphilic solution before being dried in air.

All layers formed at 23°C, while the post-treatment was performed at 50°C for 5 hours. The method used in this study is easily reproducible.

2.4. Characterization of the nanolayers

2.4.1. Water wettability study

The water repellency of the metal surfaces in the presence or absence of nanolayers was characterized by the static contact angle measured by Milli-Q water sessile drops at 20°C using a motorized syringe [14].

2.4.2. Surface visualization by atomic force microscopy

The bare and coated metal surfaces were visualized by an atomic force microscope (NanoScope III, Digital Instrument, contact operation, height and deflection mode, tip: Si_3N_4). The surface morphology was presented in 2D and 3D modes, while the three surface roughness parameters calculated by the software of the instrument were checked at three or more different places (measurement error was less than 1%).

2.4.3. Surface roughness parameters measured on the coated or uncoated surfaces of the SAM layer

Three surface roughness parameters were calculated by the software of the atomic force microscope to characterize the solid surfaces with or without nanocoatings:

R_a: the arithmetic average height that shows the absolute deviation of the irregularities to characterize the height variation;

R_q: the root mean square roughness that represents the standard deviation of the surface height distribution, while the roughness is described by a statistical method;

R_{max}: sensitive to the deep valleys and high peaks; it analyzes the profile and shows the vertical distance between the lowest valley and the highest peak [15].

2.4.4. Infrared spectroscopy

FT-IR (Fourier transform infrared) spectra were recorded on a Jasco FT/IR-4600 spectrometer equipped with a Jasco multi-reflection ATR (5 reflections), ZnSe ATR crystal (incident angle 45°) and a DTGS (deuterated-triglycine sulfate) detector used within the 4000–400 cm^{-1} range. A resolution of 4 cm^{-1} and co-addition of 128 individual spectra were applied. An ATR correction was performed on the raw spectra.

3. Results and discussion

3.1. Results of the wettability measurements

Changes in the wettability data measured on the steels with and without SAM layers are summarized in *Tables 1 and 2*. For the sake of comparison, the water contact angles measured on pure iron (ARMCO iron) are also included in *Tables 1 and 2*.

The alloying metals slightly increase the wettability of the metal samples. The presence of Mn and Mo, even at low percentages (2%), together with a lower Cr content (17%), renders this metal sample less wettable than the other one, which contains more Cr (25%) and 2% Mn. The differences are visible in the receding contact angle values on the alloys.

Table 1: Static wettability data measured on 1.4571 metal surfaces in the presence and absence of undecenyl phosphonic acid SAM layers before and after heat treatment

Solid surface	Treatment	Water contact angle (°) (advancing)	Water contact angle (°) (receding)
ARMCO iron	-	68.4	44.1
1.4571 steel	-	65.6	62.1
+4 h SAM (23°C)	-	66.9	36.7
+4 h SAM (23°C)	50°C, 5h	76.5	43.3
+24 h SAM (23°C)		72.4	43.1
+24 h SAM (23°C)	50°C, 5h	86.1	75.6
+48 h SAM (23°C)	-	79.5	47.9

Table 2: Static wettability data measured on 1.4841 metal surfaces in the presence and absence of undecenyl phosphonic acid SAM layers before and after heat treatment

Solid surface	Treatment	Water contact angle (°) (advancing)	Water contact angle (°) (receding)
ARMCO iron	-	68.4	44.1
1.4841 steel	-	60.2	57.2
+4 h SAM (23°C)	-	70.5	35.5
+4 h SAM (23°C)	50°C, 5h	73.3	45.1
+24 h SAM (23°C)		81.1	75.5
+24 h SAM (23°C)	50°C, 5h	85.5	78.3

Interestingly, the molecular layer deposition over a short period of time alters the wettability of the lower alloy steel more significantly than the other one. However, heat treatment in both cases results in the surfaces becoming more hydrophobic. A longer layer deposition time (24 h) increases the contact angles on both steels, moreover, post-heat treatment increases the surface hydrophobicity, however, the wettability does not change significantly. It is important to mention that the differences between the advancing and receding contact angles are much less in the presence of 25% Cr and 2% Mn. This means that the compactness of the layer is much more enhanced by the post-heat treatment on this alloy, a consequence of the increased surface coverage due to differences in the surface oxide composition.

3.2. Surface visualization by an atomic force microscope

In the AFM images taken of the 1.4841 steel samples shown in *Figures 1 and 2*, it can be observed that a four-hour-long immersion time in the UDP solution produces a thin layer that covers the metal surface loosely given the low receding contact angle. Increasing the immersion time results in a well-ordered layer on the metal surface that produced a special surface image. After heat treatment, the pattern on the surface does not change significantly, just the layer is more compact. By increasing the immersion time to 48 hours, the nice pattern formed earlier on the surface is still evident, but an additional layer is visible, proving that 24 h is sufficient to achieve a compact, well-ordered mono-molecular SAM layer that properly covers the steel surface.

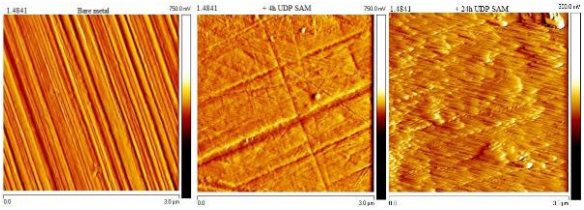

Figure 1: AFM images (taken in contact mode, visualization in deflection mode) of the starting 1.4841 steel surface and the steel with SAM nanolayers of undecenyl phosphonic acid (UDP); SAM: formed in a $5x10^{-3}$M undecenyl phosphonic acid solution at 23°C; layer formation time: 4 and 24 h

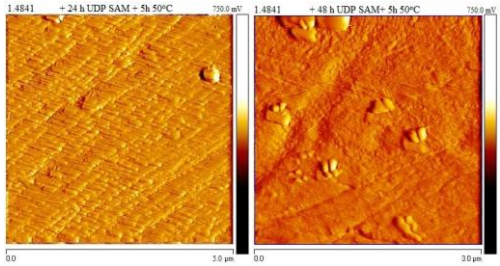

Figure 2: AFM images (taken in contact mode, visualization in deflection mode) of the starting steel surface and 1.4841 steel with self-assembled nanolayers of undecenyl phosphonic acid (UDP); SAM: formed in a $5x10^{-3}$M undecenyl phosphonic acid solution at 23°C; layer formation time: 24 and 48 h; post-heat treatment: 5 h at 50°C

These AFM images clearly show that on this steel sample a four-hour-long immersion time and post-heat treatment produce a SAM layer with a special pattern. The pattern on the layer is not altered by increasing the immersion time, however, the layer seems to be more compact. On this steel sample, the long immersion time does not result in the formation of a second layer. However, heat treatment facilitated the formation of more compact SAM layers.

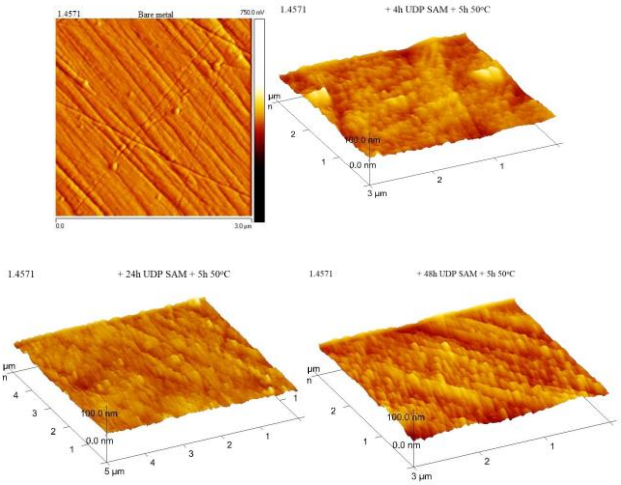

Figure 3: AFM images (taken in contact mode, visualization in deflection and 3D modes) of the 1.4571 steel surface as well as of the metal surface with self-assembled UDP nanolayers; SAM: formed in a $5x10^{-3}$M UDP solution at 23°C; layer formation time: 4, 24 and 48 h; post-treatment: 5 h at 50°C

3.3. Surface roughness parameters

The surface roughness parameters derived from the AFM images taken on coated as well as uncoated steel surfaces are summarized in *Tables 3 and 4*. The surface roughness data demonstrate well that the layer deposition – even after shorter film formation times – decreases the surface roughness. Post-heat treatment causes a small increase in these values. A visible difference in the surface roughness caused by the difference in the steel compositions is observed. More alloying components enhance the surface roughness after shorter as well as longer layer deposition times and even after heat

Table 3: Surface roughness parameters measured on uncoated and SAM layer coated surfaces of the 1.4571 alloy; R_a: arithmetic average height; R_q: root mean square roughness; R_{max}: maximum height of the profile

Solid surface	Post-heat treatment	R_q [nm]	R_a [nm]	R_{max} [nm]
ARMCO iron	-	3.21	2.34	46.2
1.4571 steel	-	7.14	5.46	58.3
+4 h SAM (23°C)	-	4.03	3.10	37.1
+4 h SAM (23°C)	50°C, 5h	5.52	4.14	49.0
+24 h SAM (23°C)		4.85	3.90	52.3
+24 h SAM (23°C)	50°C, 5h	5.41	4.09	63.7
+48 h SAM (23°C)	-	3.89	3.06	43.0

treatment. This may be a consequence of the formation of a more compact molecular film demonstrated by the contact angles.

Table 4: Surface roughness parameters measured on uncoated and SAM layer -coated surfaces of the 1.4841 alloy; R_a: arithmetic average height; R_q: root mean square roughness; R_{max}: maximum height of the profile

Solid surface	Post-heat treatment	R_q [nm]	R_a [nm]	R_{max} [nm]
1.4841 steel	-	5.22	4.17	55.6
+4 h SAM (23°C)	-	3.55	2.39	48.12
+4 h SAM (23°C)	50°C, 5h	4.71	3.36	54.9
+24 h SAM (23°C)		5.75	4.23	53.01
+24 h SAM (23°C)	50°C, 5h	6.50	4.73	63.1
+48 h SAM (23°C)	-	6.89	4.95	63.19
+48 h SAM (23°C)	50°C, 5h	7.79	5.54	78.0

3.4. Infrared spectroscopy

FT-IR spectroscopy was used to analyze the alkyl chain ordering and bonding mode of the molecules to the surface. On the polished, that is, cleaned stainless steel substrates, no sign of organic deposition was observed from their spectra.

In the spectra of SAM layer deposited substrates, the reference peaks determine that the organization of SAMs was defined by the C-H stretching vibrations of the methylene group. The C-H stretching possesses two typical stretching vibrations: antisymmetric represented by a peak at 2850 cm^{-1} and asymmetric stretching represented by a peak at 2918 cm^{-1}. The frequency of these two wavenumbers becomes either higher or lower depending on the conformation of the alkyl chain. When the peaks are centered at wavenumbers that are shifted to higher frequencies ($\nu_{asym}CH_2 > 2918$ cm^{-1}), a disordered monolayer with gauche defects in the alkyl chain is suggested. Conversely, if the wavenumbers shift to lower frequencies, the monolayer is considered to be ordered ($\nu_{asym}CH_2 < 2918$ cm^{-1}) with all-trans C-C bonds. In this study, the peaks corresponding to CH_2 were positioned at $\nu_{asym}CH_2 = 2917.7$ and $\nu_{sym}CH_2 = 2850.5$ cm^{-1}, while those concerning undecenyl phosphonic acid were shifted to 2920.3 and 2850.1 cm^{-1} in the spectrum of its SAM layer on the 1.4841 steel surface. The 2.6 cm upshift of the antisymmetric CH_2 stretching band indicates the formation of a slightly disordered surface structure with some *gauche* conformations in the alkyl chain (*Figure 4*). Meanwhile, an insignificant 0.4 cm^{-1} downshift of the symmetric CH_2 stretching band was observed. Besides these effects, it was observed that the band broadened slightly. The two CH_2 stretching bands exhibit 21 and 14 cm^{-1} half band half widths in the spectrum of undecenyl phosphonic acid, which were slightly broadened to 23 and 16 cm^{-1} for antisymmetric and symmetric CH_2 stretching bands in the SAM layer, respectively.

Additional information regarding the bonding of the head group to the substrate can be obtained by analyzing the position of the IR absorption bands in the fingerprint region. *Figure 5* and *Table 5* show the selected IR bands important for structural and compositional characterization of the formed SAM layer.

The assignment of fingerprint regions is especially difficult due to the appearance of various deformation modes of CH_2 groups, namely scissoring, wagging, twisting and rocking modes, as well as the alkyl chain C-C stretching modes.

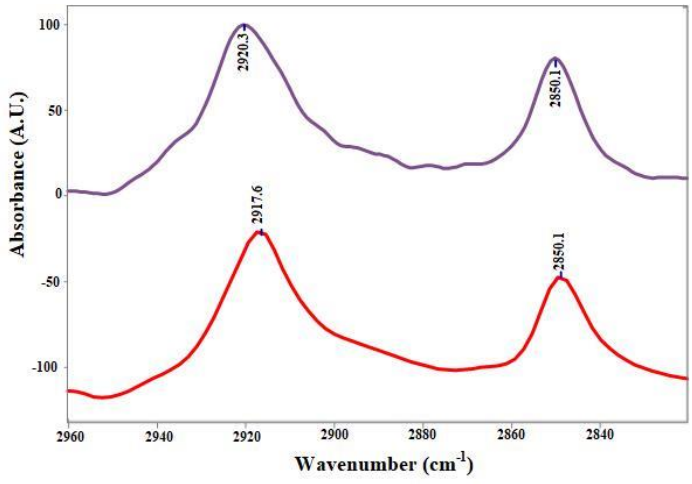

Figure 4: IR spectra of undecenyl phosphonic acid (lower trace) and its SAM layer on the 1.4841 steel surface in the CH_2 stretching band (upper trace). The precise positions of the bands were obtained by calculating their second derivatives $\nu_{asym}CH_2 = 2920.3$ and $\nu_{sym}CH_2 = 2850.1$ cm^{-1}, indicating the presence of a strongly bound and ordered film

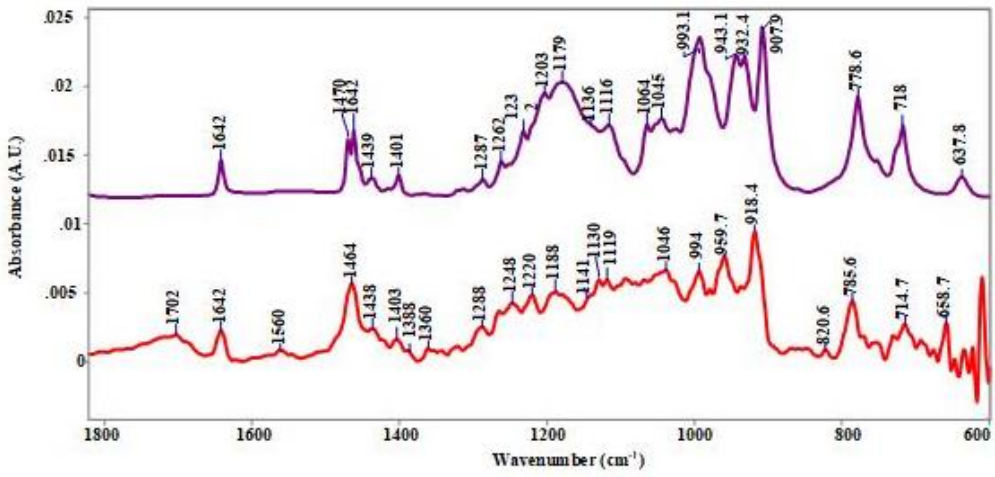

Figure 5: IR spectra of undecenyl phosphonic acid (upper trace) and the SAM layer on the 1.4841 steel surface (lower trace) in the fingerprint region

Two extra bands were detected at 1702 and 1560 cm^{-1} assigned to partial oxidation of the product, that is, ketones and antisymmetric stretching of the carboxylate group vibrational mode, respectively. Two weak bands result from symmetric COO^- stretching at 1388 and 1360 cm^{-1}.

All four characteristic bands of olefinic end groups, namely C=C stretching, $=CH_2$ scissoring, $=CH_2$ wagging and $=CH_2$ rocking, can be seen in the IR spectrum of the SAM layer.

Insignificant frequency shifts were observed in symmetric (β_sPOH) and antisymmetric (β_aPOH) P-O-H in-plane bending modes. The DPU exhibits bands at 1136 and 1116 cm^{-1}, while the studied SAM layer yields bands at 1130 and 1119cm^{-1}. A very similar effect was observed in the case of out-of-plane P-O-H deformations. The symmetric (γ_sPOH) and antisymmetric (γ_aPOH) out-of-plane deformation bands appeared at 779 and 718 cm^{-1} in the IR spectrum of UDP, moreover, these features only slightly shifted in the case of heated SAMs, e.g., to 786 and 715 cm^{-1}. From these experimental results, it can be concluded that the $–P(OH)_2$ side of the phosphoryl group did not strongly interact with the metal surface.

Additional information regarding the bonding of the head group to the substrate can be obtained by analyzing the position of the IR absorption bands in the P=O stretching region (1000-1200 cm^{-1}) for phosphonic acids. Although the interpretation of the peaks within this region is hindered by their broadness and complexity, the substantial variations observed provide compelling evidence for the existence of a robust interaction between the phosphonate head group and the oxidized metal surface. The difference between the starting spectrum of undecenyl phosphonic acid and those of the films on the metal surface is very significant. The most significant difference is observed in the intense valence vibrations of the phosphoryl group. A major effect of surface bounding was that the unbounded P=O stretching at 1179 cm^{-1} downshifted to 1046 cm^{-1}. In contrast to the P-O single bond stretching of $–P(OH)_2$, strong bands of the UDP–$P=O(OH)_2$ end group at 938 and 908 cm^{-1} correspond to the $-PO_2$ asymmetric and $-PO_2$ symmetric stretching vibrations, respectively, which are only slightly upshifted in the IR spectrum of SAM layer on the 1.4841 steel surface to 960 and 918 cm^{-1}. According to these relatively small shifts in P-O stretching bands in agreement with the little shifts of the P-O-H deformation features, it can be concluded that in the $–P=O(OH)_2$ end group, the $–P(OH)_2$ site weakly interacts with the metal surface. Contact with the metal surface is most significant at the –P=O site of the $–P=O(OH)_2$ end group exhibiting about a 130 cm^{-1} downshift on the metal surface.

Besides the aforementioned experimental observations, some weak features among the aliphatic CH_2 deformation modes can be assigned to the partial presence of *gauche* conformers in the long chain (see *Table 5*).

To summarize the infrared spectroscopic results, the precise analysis of spectra taken in UDP in bulk and in nanolayer forms proved that the amphiphilic monomers in SAM layers yield different spectra from the bulk one. Additionally, the detailed analysis of the fingerprint region of the spectra demonstrated clearly how the head group of the amphiphile ($-P(O)(OH)_2$) is bound to the metal/metal oxide surface (mostly through the metal oxide layers) as well as demonstrated the interaction between the hydrophobic chains. Similar results were observed on the heat-treated UDP in bulk and nanolayer forms.

4. Conclusion

The alloying metals slightly increase the wettability of the metal samples. The presence of Mn and Mo, even at low percentages (2%), together with a lower Cr content (17%) results in similar contact angles to the other steel,

Table 5: Comparison of selected infrared bands from ATR spectra of the $H_2C=CH-(CH_2)_9PO(OH)_2$ molecule of the original powdered sample and heat-treated SAM layer sample after 24 hours of heating at 50°C.

bulk powder at 25°C	SAM layer at 50°C for 24h	Assignments	Remarks
2917.7 vs (a)	2920.3 vs (b)	ν_aCH_2	
2850.5 s	2850.1 vs	ν_sCH_2	
-	1702 w,b	$\nu C=O$	Oxidation products
-	1560 w	ν_aCOO^-	
1642 m	1642 m	$\nu C=C$	
1401 m,w	1403 w	$\delta = CH_2$	
993 vs	994 s	$\omega = CH_2 + \nu P=O$	
638 w	659 w	$\rho = CH_2$ (vinyl) + $\gamma = CH$	
1470 m,s		δCH_2	(*trans*)
1462 m,s	1468 s	δCH_2	(*gauche*)
	1388 vw / 1360 vw	ν_sCOO^-	Oxidation products
1136 w,sh	1130 w	β_sPOH	
1116 m	1119 w	β_aPOH	
1179 vs	1188 m	$\nu P=O$	(unbounded)
	1046 m	$\nu P=O$	(surface bounded)
-	1141 vw	tCH_2	(*gauche*)
938 s (doublet)	960 s	ν_aPO_2	
908 s	918 s	ν_sPO_2	
-	821 vw	$\rho CH_2 + \gamma_sPOH$	(*gauche*)
779 s	786 s	γ_sPOH	
718 s	715 m	γ_aPOH	

Remarks:

[a] Abbreviations used to describe the intensity and shape of bands: vs = very strong; s = strong; m = moderate; w = weak; vw = very weak; b = broad; and sh = shoulder.

[b] The proposed assignments were taken from DFT calculations [16] and the following notations used for different vibrational modes: ν = stretching; δ = deformation or scissoring; ω = wagging; t = twisting; ρ = rocking; β = in-plane deformation; and γ = out-of-plane deformation modes.

which contains Cr at a higher concentration (25%) as well as 2% Mn. The differences are not significant. The heat treatment causes a significant increase in the contact angles. The increased level of compactness is proved by the smaller differences in the advancing and receding contact angles.

A longer layer deposition time (24 h) increases the water contact angles on both steels, even before and after post-heat treatment.

The metal surfaces, with and without self-assembled molecular layers imaged by a atomic force microscope, showed that the formation of nanolayers changes the surface morphology significantly.

The surface roughness parameters demonstrate that layer deposition – even after shorter film formation times – decreases the surface roughness. Post-heat treatment causes a small increase in these values. A visible difference in the surface roughness caused by the difference in the steel compositions is observed. More alloying components enhance the surface roughness over shorter and longer layer deposition times as well as after heat treatment, which may be a consequence of the differences in the layer compositions of the oxide surface.

Differences between spectra of undecenyl phosphonic acid measured on the bulk material and involved in nanolayers were proven by infrared spectroscopic measurements. Furthermore, bonding between the phosphonic acid head groups and the solid surface (mainly via the metal oxides) as well as hydrophobic interactions between the alkenyl groups were clearly demonstrated.

Experiments on the layer thickness by spectroscopic ellipsometry as well as the determination of the composition of the oxide surface by XPS are in progress.

Acknowledgements

The authors are grateful for the experimental support provided by László Trif (Research Centre for Natural Sciences) and Péter Márton (Budapest University of Technology and Economics).

REFERENCES

[1] Dhaundiyal, P.; Bashir, S.; Sharma, V.; Kumar, A.: An investigation on mitigation of corrosion of mildsteel by Origanum vulgare in acidic medium, *Bull. Chem. Soc. Ethiop.*, 2019, 33(1), 1, DOI: 10.4314/bcse.v33i1.16

[2] Mouden, O.I.E.; Ahmed, B.; Bammou, L.; Belkhaouda, M.; Anejjar, A.; Salghi, R.: Zygophyllum qatarense extract as corrosion inhibitor for mild steel in acidic medium, *Appl. J. Environ. Eng. Sci.*, 2021, **7**(1), 114–124, DOI: 10.48422/IMIST.PRSM/ajees-v7i1.25727

[3] Karthik, B.B.; Selvakumar, P.; Thangavelu C.: Phosphonic acids used as corrosion inhibitors - a review, *Asian J. Chem.*, 2012, **24**(8), 3303–3308, AJC-11132

[4] Yurt, A.; Solmaz, E.: Phosphonic acid monolayers for corrosion protection of copper: EQCM and EIS investigations, *Surf. Rev. Lett.*, 2020, **27**(06), 1950166-1–1950166-16, 2020, DOI: 10.1142/S0218625X1950166X

[5] Herbáth, B.; Kovács, K.; Jakab, M.: The effect of different accelerators on the corrosion protection of a surface coating on spheroidal graphite cast iron (Ductile Iron), *Hung. J. Ind. Chem*., 2023 **51**(1) 43–53, DOI: 10.33927/hjic-2023-07

[6] Telegdi, J.; Luciano, G.; Mahanty, S.; Abohalkuma, T.: Inhibition of aluminum alloy corrosion in electrolytes by self-assembled fluorophosphonic acid molecular layer, *Mater. Corros*., 2016, **67**(10), 1027–1033, DOI: 10.1002/maco.201508792

[7] Abohalkuma, T.; Telegdi, J.: Corrosion protection of carbon steel by special phosphonic acid nano-layers, *Mater. Corros*., 2015, **66**(12), 1382–1390, DOI: 10.1002/maco.201508304

[8] Kanta, A.; Sedev, R.; Ralston, J.: The formation and stability of self-assembled monolayers of octadecylphosphonic acid on titania, *Colloids Surf. A Physicochem. Eng. Asp.*, 2006, **291**(1–3), 51–58, DOI: 10.1016/j.colsurfa.2005.12.057

[9] Kristan Mioč, E.; Hajdari Gretić, Z.; Otmačić Ćurković, H.: Modification of cupronickel alloy surface with octadecylphosphonic acid self–assembled films for improved corrosion resistance, *Corros. Sci.*, 2018, **134**, 189–198, DOI: 10.1016/j.corsci.2018.02.021

[10] Kuznetsov, Y.I.: Organic corrosion inhibitors: where are we now? A review. Part IV. Passivation and the role of mono- and diphosphonates, *Int. J. Corros. Scale Inhib.*, 2017, **6**(4), DOI: 10.17675/2305-6894-2017-6-4-3

[11] Nhiem, L.T.; Oanh, D.T.Y.; Hieu, N.H.: Nanocoating toward anti-corrosion: A review, *Vietnam J. Chem.*, 2023, **61**(3), 284–293, DOI: 10.1002/vjch.202300025

[12] Saji, V.S.; Thomas, J.: Nano-materials for corrosion control, *Curr. Sci.*, 2007, **92**(1), 51–55, http://www.jstor.org/stable/24096821

[13] Neves, B.R.A.; Salmon, M.E.; Russell, P.E.; Troughton, E.B.: Thermal Stability Study of Self-Assembled Monolayers on Mica, *Langmuir*, 2000, **16**(6), 2409–2412, DOI: 10.1021/la990648t

[14] Románszki, L.; Mohos, M.; Telegdi, J.; Keresztes, Z.; Nyikos, L.: A comparison of contact angle measurement results obtained on bare, treated, and coated alloy samples by both dynamic sessile drop and Wilhelmy method, *Period Politech-Chem*, 2014, **58**(Supplement), 53–59, 2014, DOI: 10.3311/PPch.7188

[15] Gadelmawla, E.S.; Koura, M.M.; Maksoud, T.M.A.; Elewa, I.M.; Soliman, H.H.: Roughness parameters, *J. Mater. Process. Technol.*, 2002, **123**(1), 133–145, DOI: 10.1016/S0924-0136(02)00060-2

[16] Pfeifer, É.K.; Telegdi, J.; Mihály, J.; Németh, Cs.; Drees, M.; Hajba, L.; Mink, J.: Vibrational spectroscopic and theoretical study of undecenyl phosphonic acid for understanding its structure and bonding properties in self-assembling molecular layers formed on various types of steel surfaces, *Appl. Spectrosc. Rev.* (under publication)